Tomographic cross-correlation of the CMB gravitational lensing and galaxy clustering - effect of photometric redshift errors

Paweł Bielewicz

NARODOWE CENTRUM BADAŃ JĄDROWYCH ŚWIERK

Collaborator: Chandra Shekhar Saraf

CMB gravitational lensing

- Deflection of the CMB photon paths by the large-scale structure of the Universe (~ 3')
- Correlation of deflection angles over the sky by an angle ~ 2°
- Reconstruction of lensing potential from changes in CMB anisotropy
- Lensing potential as a tracer of dark matter distribution

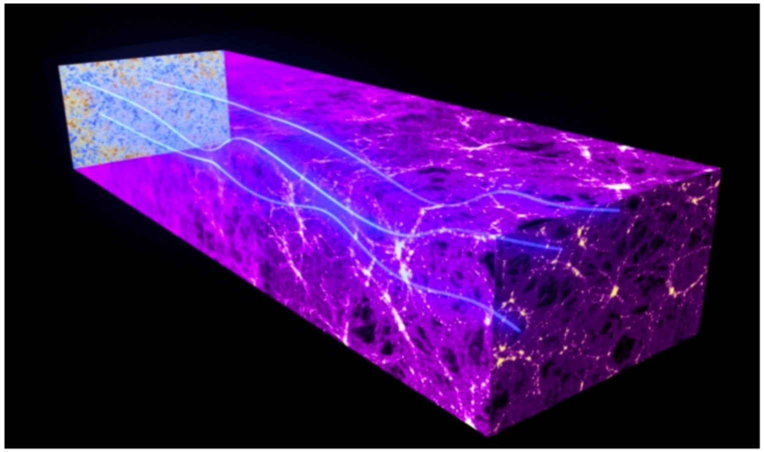

$$\phi(\hat{n}) = -\frac{2}{c^2}\int_0^{\chi_{rec}} d\chi \frac{D_{ls}}{D_l D_s}\Psi(\chi_0 - \chi, \chi\hat{n})$$

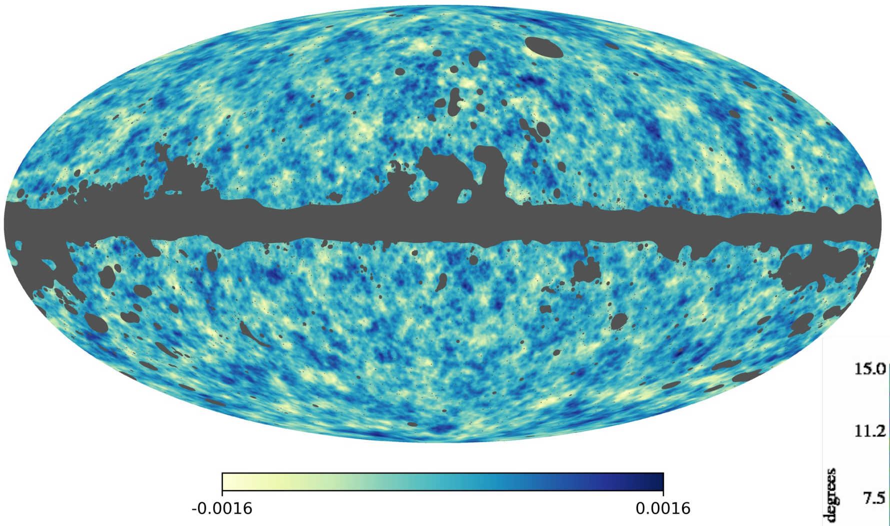

Planck collaboration et al. (2020)

$$\Delta\widetilde{T}(\hat{n}) = \Delta T(\hat{n} + \nabla\phi(\hat{n}))$$

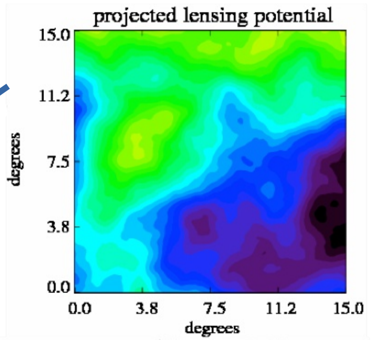

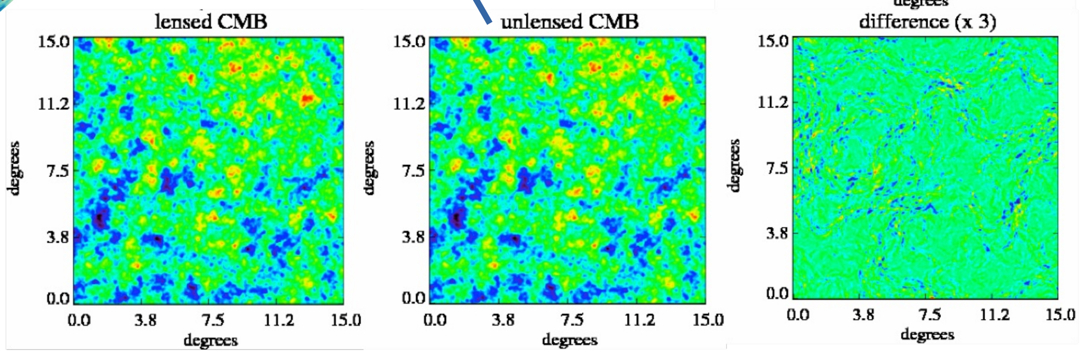

Cross-correlation between CMB lensing and galaxy surveys

- Broad CMB lensing kernel does not allow tracing time evolution of dark matter clustering

$$\phi(\hat{n}) = -\frac{2}{c^2}\int_0^{\chi_{rec}} d\chi \frac{D_{ls}}{D_l D_s}\Psi(\chi_0 - \chi, \chi\hat{n})$$

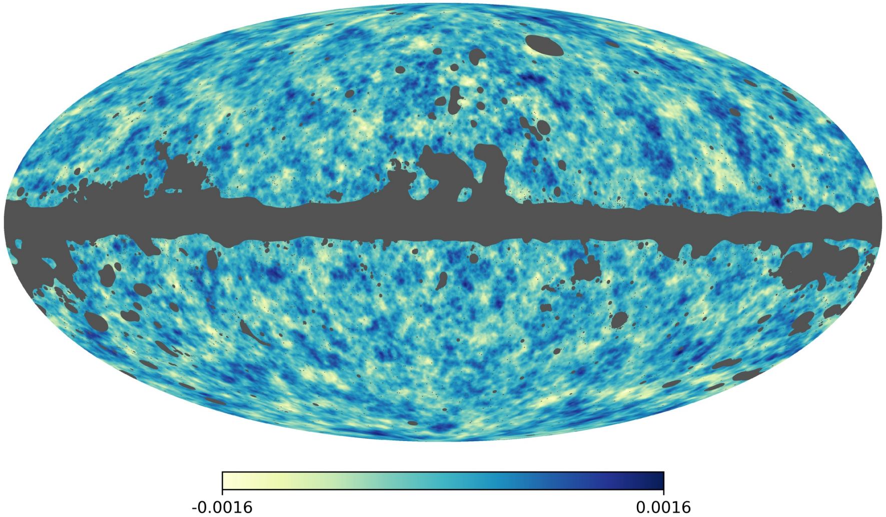

Planck collaboration et al. (2020)

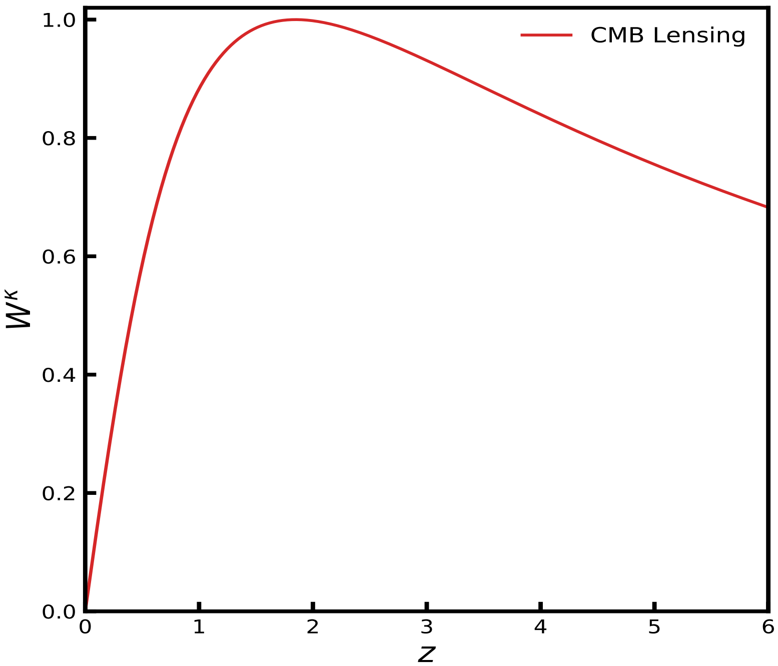

Cross-correlation between CMB lensing and galaxy surveys

- Broad CMB lensing kernel does not allow tracing time evolution of dark matter clustering
- Needed cross-correlation of CMB lensing map with objects with known redshift (galaxies, quasars, radio sources, etc.)
- Splitting redshift distribution on redshift bins (cosmic tomography: White et al. 2022; Pandey et al. 2022; Chang et al. 2022; Sun et al. 2022; Krolewski et al. 2021; Hang et al. 2021; Peacock & Bilicki 2018, Saraf et al. 2024)
- How **photo-z errors** affect estimation of angular power spectra and cosmological parameters?

$$\phi(\hat{n}) = -\frac{2}{c^2}\int_0^{\chi_{rec}} d\chi \frac{D_{ls}}{D_l D_s}\Psi(\chi_0-\chi, \chi\hat{n})$$

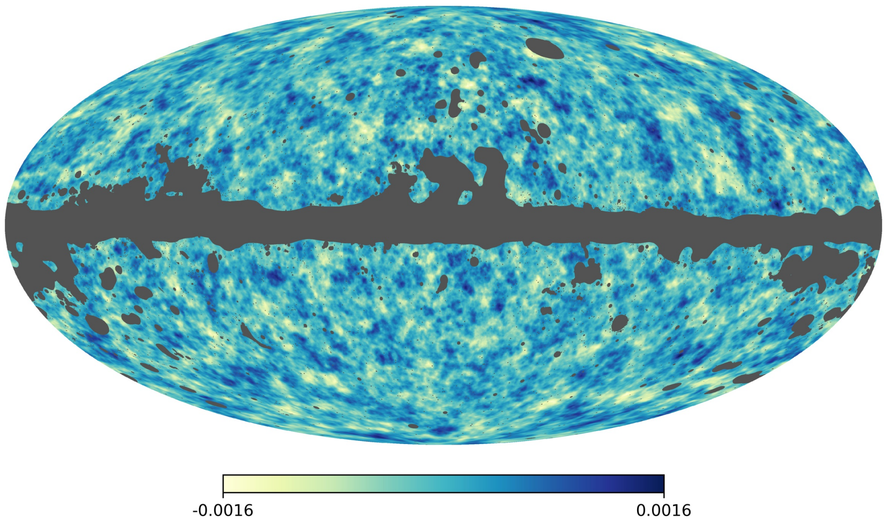

Planck collaboration et al. (2020)

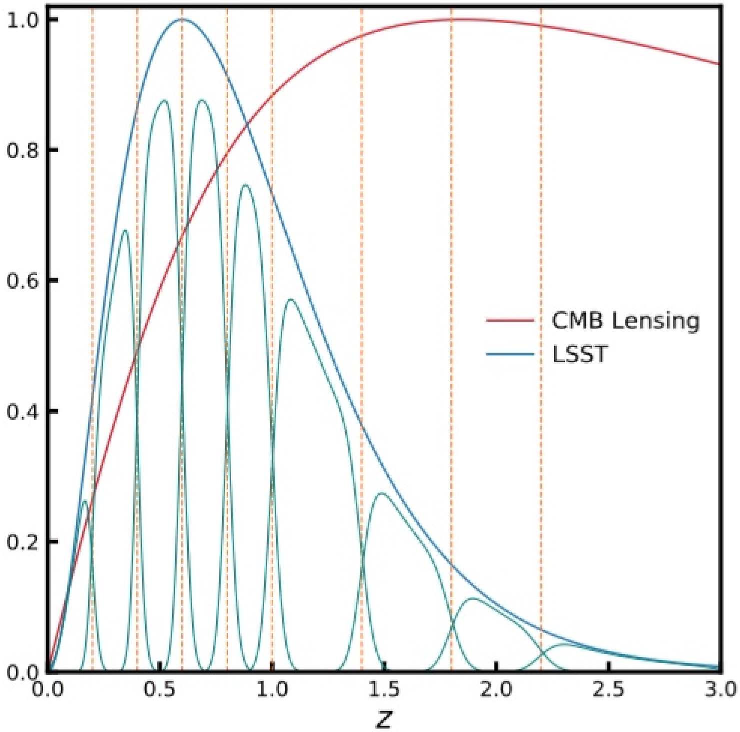

Saraf, PB (2024)

Cross-correlation power spectrum

- Estimation of σ_8 and galaxy bias parameters from the angular power spectra of the lensing potential and galaxy distribution
- Cross-power spectrum between CMB lensing and galaxy density contrast

$$C_\ell^{\kappa g} = \int_0^{\chi_*} \mathrm{d}\chi \frac{W^\kappa(\chi)\, W^g(\chi)}{\chi^2}\, P_m\left(k = \frac{\ell + 1/2}{\chi}, z(\chi)\right) \qquad \theta \sim \frac{\pi}{\ell}$$

$$\kappa(\hat{\mathbf{n}}) = -\frac{1}{2}\nabla^2\phi(\hat{\mathbf{n}})$$

$$g = \frac{n - \bar{n}}{\bar{n}}$$

$$W^\kappa(\chi) = \frac{3\,\Omega_m}{2\,c^2} H_0^2 (1+z)\,\chi\,\frac{\chi_* - \chi}{\chi_*}$$

$$\mathrm{W}^g(\chi) = b(z(\chi))\,\frac{H(\chi)}{c}\,\frac{\mathrm{d}N}{\mathrm{d}z(\chi)}$$

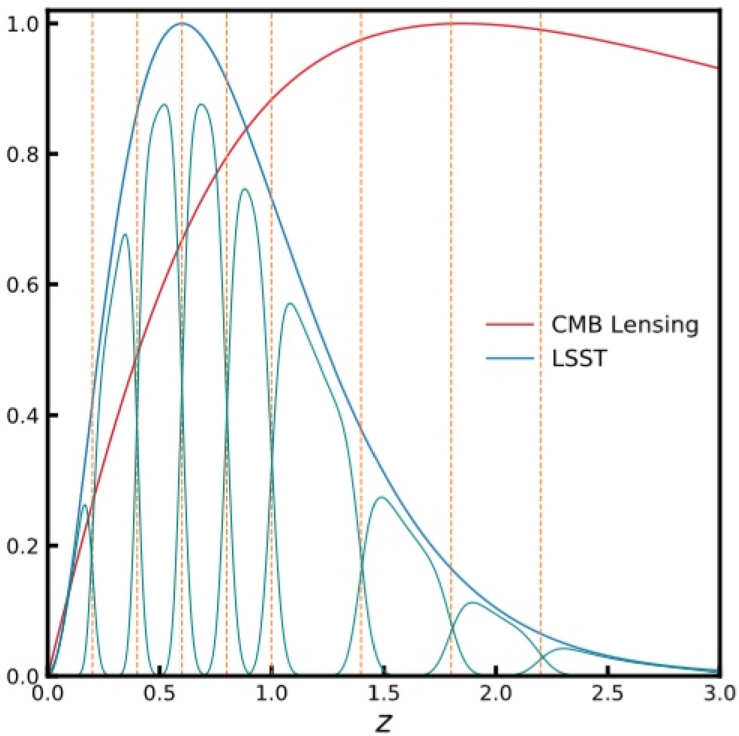

Testing tomographic cross-correlation

- Test using simulations of LSST galaxy survey
- 300 simulations of correlated log-normal galaxy over-density (with LSST Science Book redshift distribution) and CMB lensing convergence fields (consistent with Planck CMB lensing map) using Full-sky Lognormal Astro-fields Simulation Kit (FLASK) code (Xavier et al. 2016)

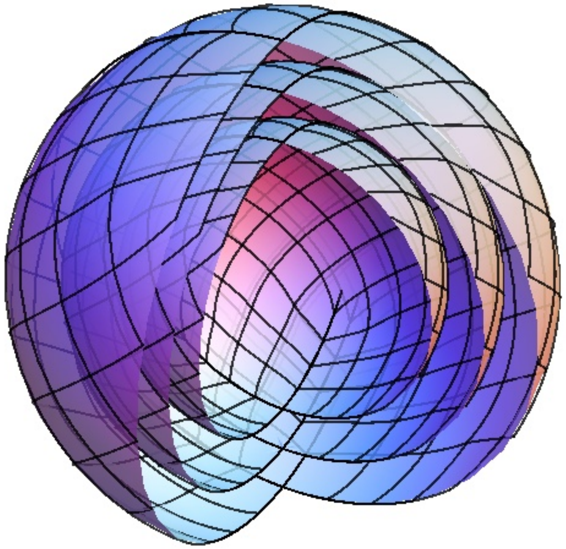

Tomographic binning of redshift distribution

- Photometric redshifts z_p obtained by adding gaussian or lorentzian photo-z errors to true redshifts z_t

$$\frac{\mathrm{d}N(z_p)}{\mathrm{d}z_p} = \int \mathrm{d}z_t \frac{\mathrm{d}N(z_t)}{\mathrm{d}z_t} p(z_p - z_t | z_t)$$

$$p(z_p - z_t|z_t) = \mathcal{G}(z_t, \sigma(z_t))$$
$$\sigma(z) = \sigma_0(1+z)$$

$$p(z_p - z_t|z_t) \propto \left[1 + \frac{1}{2a}\left(\frac{z_p - z_t}{\gamma_0(1+z_t)}\right)^2\right]^{-a}$$

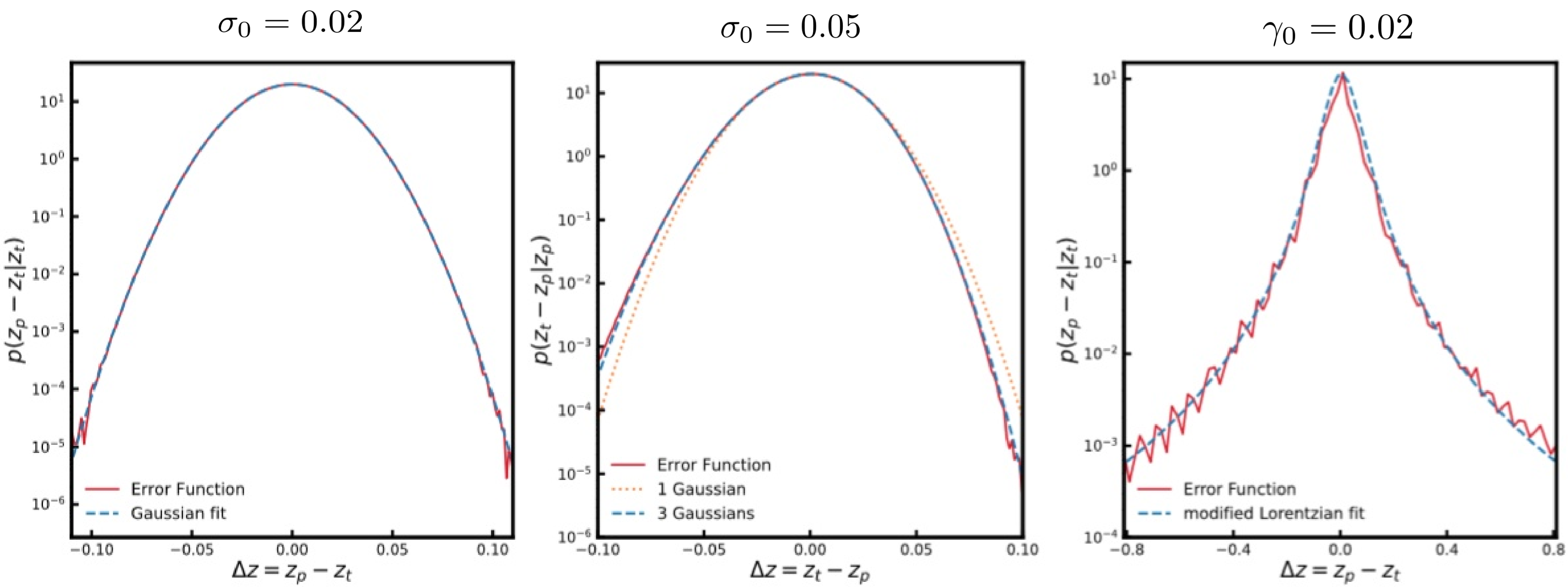

Saraf, PB (2024)

Tomographic binning of redshift distribution

- Photometric redshifts z_p obtained by adding gaussian or lorentzian photo-z errors to true redshifts z_t

$$\frac{dN(z_p)}{dz_p} = \int dz_t \frac{dN(z_t)}{dz_t} p(z_p - z_t | z_t)$$

- Tomographic binning of the true redshift distribution

$$\frac{dN^i(z_p)}{dz_p} = \int dz_t \frac{dN(z_t)}{dz_t} W^i(z_t) p^i(z_p - z_t | z_t) \qquad W^i(z_t) = \begin{cases} 1, & \text{if} \quad z^i_{\rm min} \le z_t < z^{i+1}_{\rm min} \\ 0, & \text{otherwise} \end{cases}$$

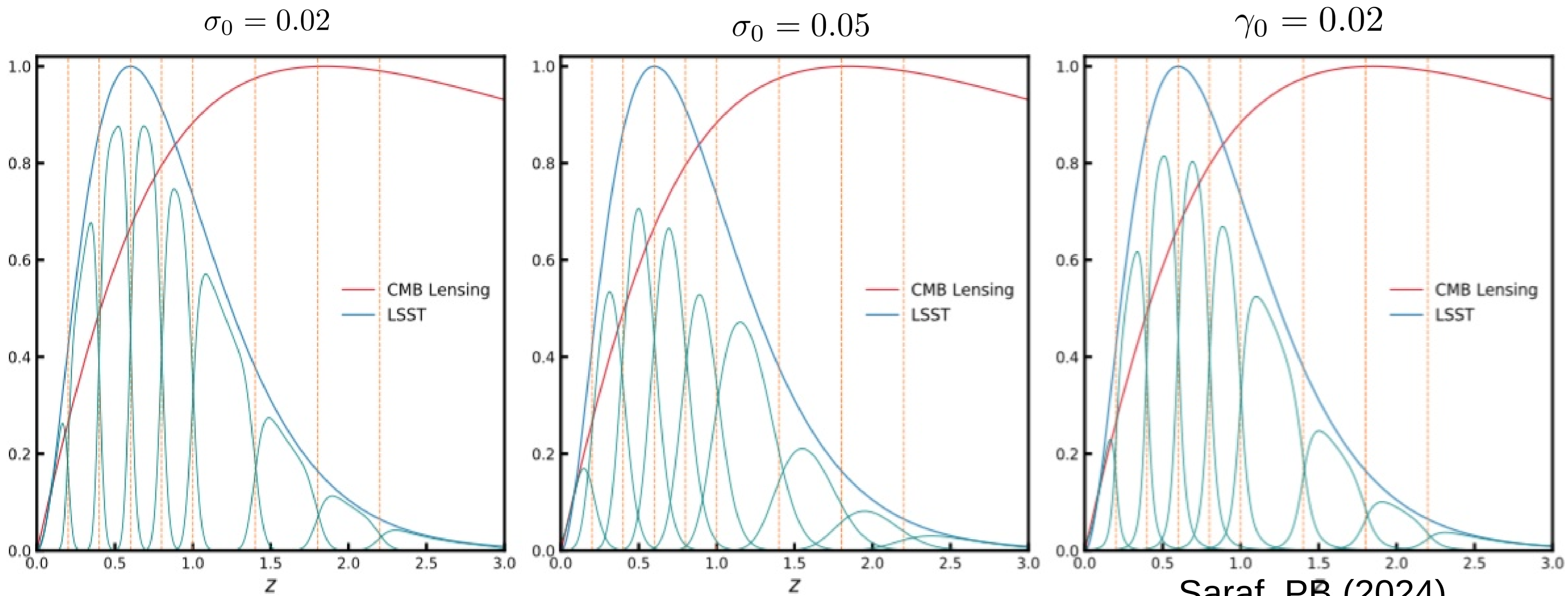

Saraf, PB (2024)

Tomographic binning of redshift distribution

- Photometric redshifts z_p obtained by adding gaussian or lorentzian photo-z errors to true redshifts z_t

$$\frac{dN(z_p)}{dz_p} = \int dz_t \frac{dN(z_t)}{dz_t} p(z_p - z_t | z_t)$$

- Tomographic binning of the true redshift distribution

$$\frac{dN^i(z_p)}{dz_p} = \int dz_t \frac{dN(z_t)}{dz_t} W^i(z_t) p^i(z_p - z_t | z_t) \qquad W^i(z_t) = \begin{cases} 1, & \text{if } z^i_{\min} \le z_t < z^{i+1}_{\min} \\ 0, & \text{otherwise} \end{cases}$$

- Simple model of power spectra for galaxies with photo-z

$$C_i^{gg,ph}(\ell) = \int_0^{\chi_*} \frac{d\chi}{\chi^2} \left(b(z_p) \frac{dN^i(z_p)}{dz_p} \right)^2 P_m \left(k = \frac{\ell + 1/2}{\chi}, z_p(\chi) \right)$$

$$C_i^{\kappa g,ph}(\ell) = \int_0^{\chi_*} \frac{d\chi}{\chi^2} W^\kappa(\chi)\, b(z_p) \frac{dN^i(z_p)}{dz_p} P_m \left(k = \frac{\ell + 1/2}{\chi}, z_p(\chi) \right)$$

Power spectra for tomographic analysis

- Power spectra for galaxies with photometric redshifts are related to power spectra for galaxies with true redshifts by (Zhang et al. 2010):

$$C_{ij}^{gg,ph}(\ell) = \sum_k P_{ki}\, P_{kj}\, C_{kk}^{gg,tr}(\ell)$$

$$C_{i}^{\kappa g,ph}(\ell) = \sum_k P_{ki}\, C_{kk}^{\kappa g,tr}(\ell)$$

where $P_{ij} \equiv \frac{N_{i\to j}}{N_j^{ph}}$ is so called scattering matrix ($\sum_i P_{ij} = 1$)

$$C_{kk}^{gg,tr}(\ell) = \int_0^{z_*} \frac{\mathrm{d}z_t}{c} \frac{H(z_t)}{\chi^2(z_t)} \left(b(z_t) \frac{dN(z_t)}{dz_t} \right)^2 W^k(z_t)\, P_m\left(k = \frac{\ell + 1/2}{\chi(z_t)}, z_t\right)$$

$$C_{kk}^{\kappa g,tr}(\ell) = \int_0^{z_*} \frac{\mathrm{d}z_t}{c} \frac{H(z_t)}{\chi^2(z_t)} W^\kappa(z_t)\, b(z_t) \frac{dN(z_t)}{dz_t} W^k(z_t)\, P_m\left(k = \frac{\ell + 1/2}{\chi(z_t)}, z_t\right)$$

Power spectra for tomographic analysis

- Power spectra for galaxies with photometric redshifts are related to power spectra for galaxies with true redshifts by (Zhang et al. 2010):

$$C_{ij}^{gg,ph}(\ell) = \sum_k P_{ki}\, P_{kj}\, C_{kk}^{gg,tr}(\ell)$$

$$C_{i}^{\kappa g,ph}(\ell) = \sum_k P_{ki}\, C_{kk}^{\kappa g,tr}(\ell)$$

where $P_{ij} \equiv \dfrac{N_{i\to j}}{N_j^{ph}}$ is so called scattering matrix ($\sum_i P_{ij} = 1$)

- Zhang et al. (2017) proposed algorithm, Non-negative Matrix Factorization, to solve

  for P_{ij} and $C_{kk}^{tr}(\ell)$ having $C_{ij}^{ph}(\ell)$

- With estimation of the true redshift distribution it is possible fast method of computation of the scattering matrix

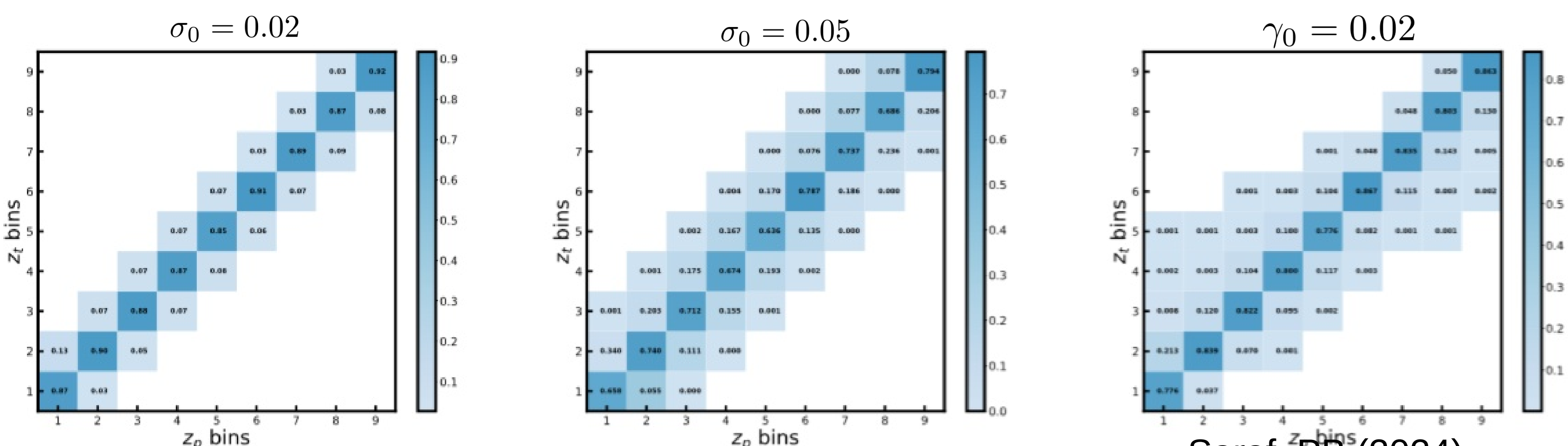

Saraf, PB (2024)

NARODOWE CENTRUM BADAŃ JĄDROWYCH ŚWIERK

Tests for simulations without correction for photo-z errors

- Estimation of the angular power spectra

$$\hat{C}_L^{xy} = \sum_{L'} K_{LL'}^{-1} \left(\tilde{C}_{L'}^{xy} - \left\langle \tilde{N}_{L'}^{xy} \right\rangle_{MC} \right) \qquad \tilde{C}_\ell^{xy} = \frac{\sum_m \tilde{a}_{\ell m}^{x} \tilde{a}_{\ell m}^{y*}}{2\ell + 1}$$

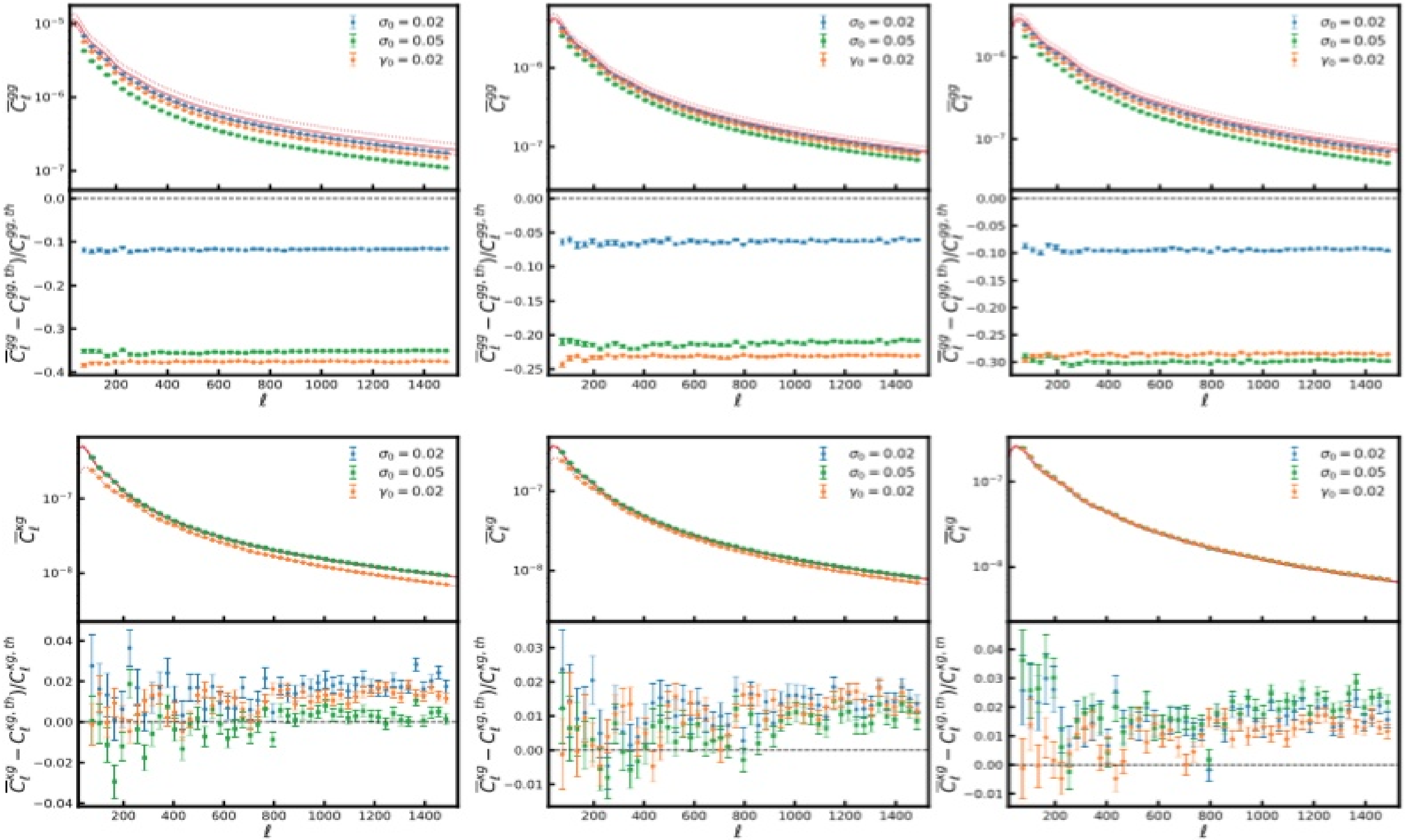

Bin 5 ($0.8 \leq z < 1.0$) Bin 6 ($1.0 \leq z < 1.4$) Bin 7 ($1.4 \leq z < 1.8$)

Saraf, PB (2024)

Tests for simulations after correction for photo-z errors

- Estimation of the angular power spectra

$$\hat{C}_L^{xy} = \sum_{L'} K_{LL'}^{-1} \left(\tilde{C}_{L'}^{xy} - \left\langle \tilde{N}_{L'}^{xy} \right\rangle_{MC} \right) \qquad \tilde{C}_\ell^{xy} = \frac{\sum_m \tilde{a}_{\ell m}^x \tilde{a}_{\ell m}^{y*}}{2\ell + 1}$$

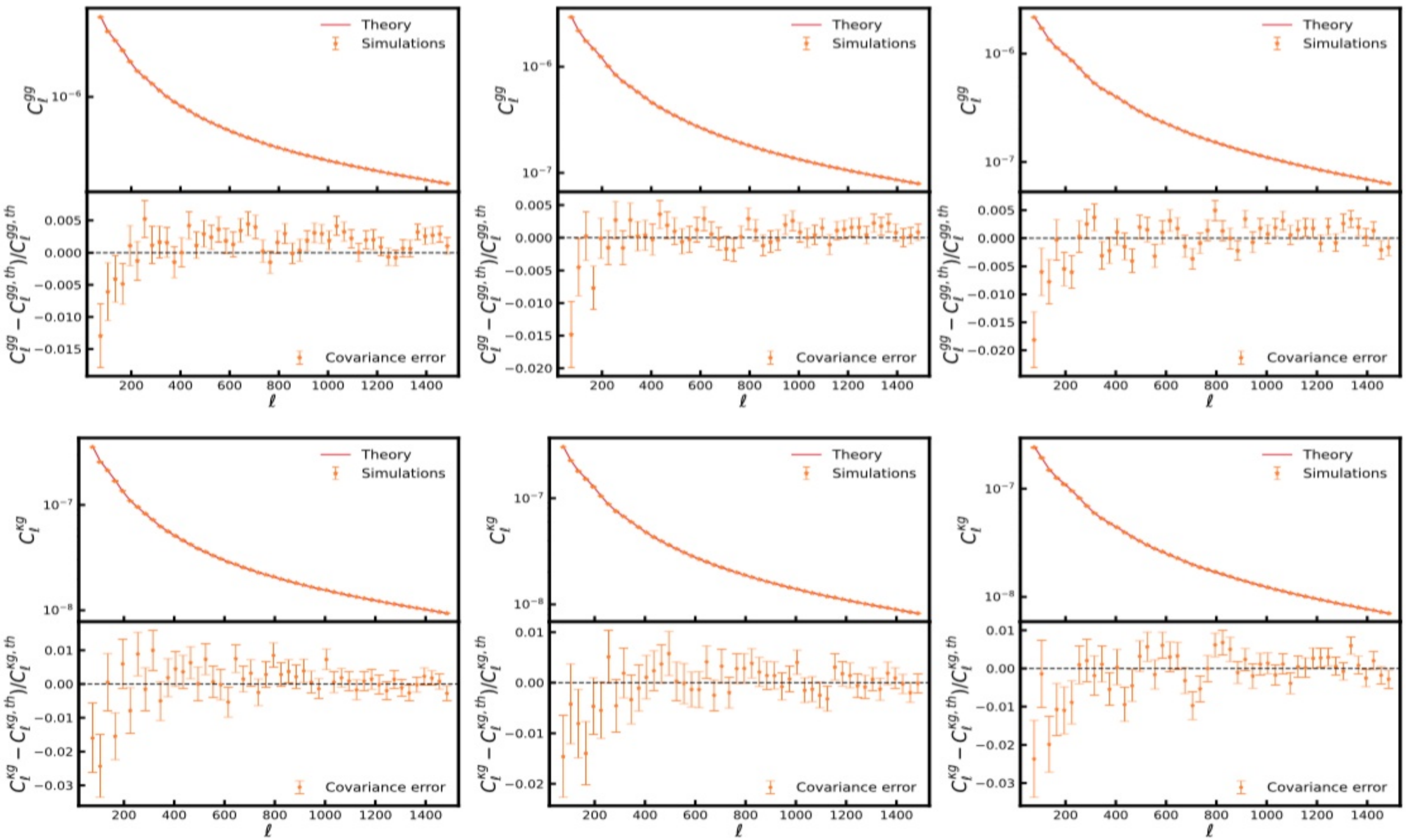

Bin 5 ($0.8 \le z < 1.0$) **Bin 6 ($1.0 \le z < 1.4$)** **Bin 7 ($1.4 \le z < 1.8$)**

Saraf, PB (2024)

Estimation of the parameters

$$\sigma_8(z) = A(z)\,\sigma_{8,0}\,D(z)$$

$\sigma_0 = 0.02$ $\sigma_0 = 0.05$ $\gamma_0 = 0.02$

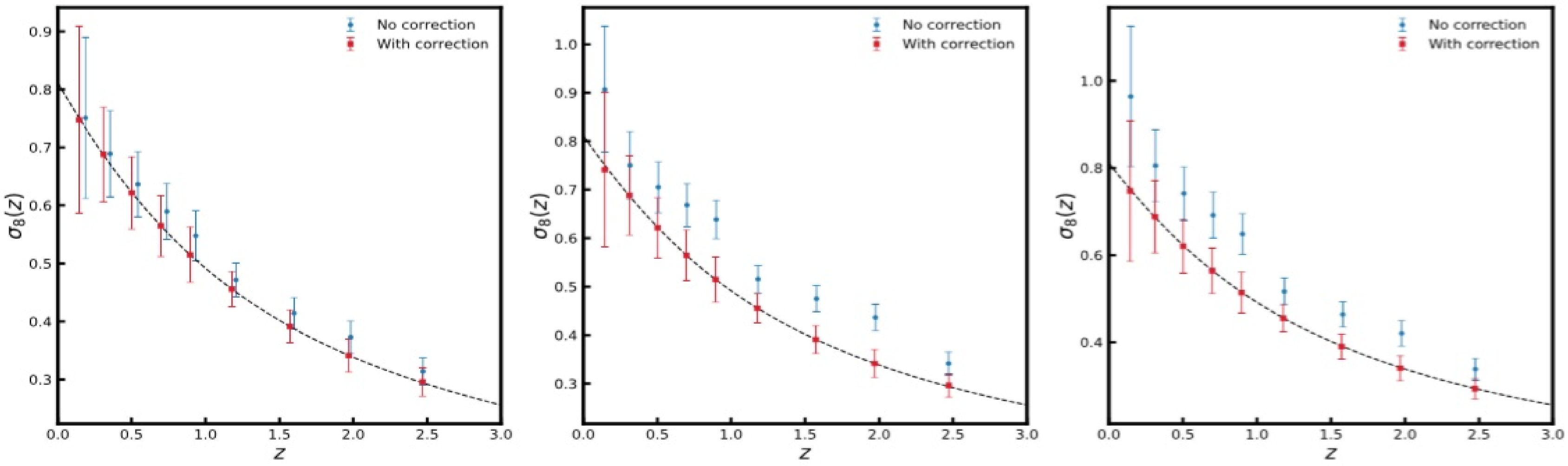

Saraf, PB (2024)

LSST simulations

- Redshift Assessment Infratructure Layers (RAIL)
- Redshifts and six band magnitudes from Buzzard simulations (DeRose et al. 2019)
- Added errors on photometric magnitudes consistent with LSST Y1
- Photo-z estimated using FlexZBoost
- Added correlations with CMB using GLASS (Tessore et al. 2023)

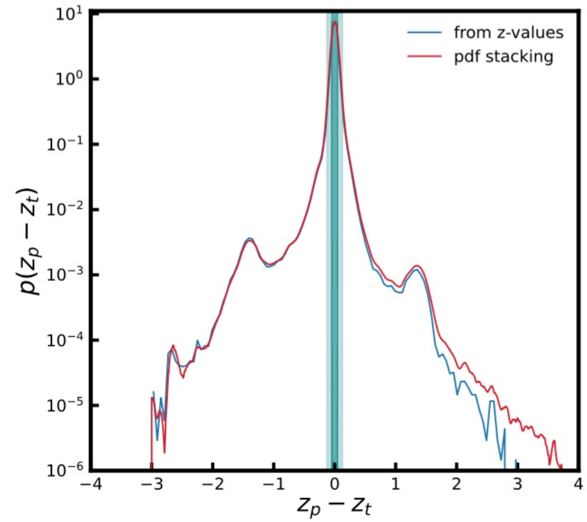

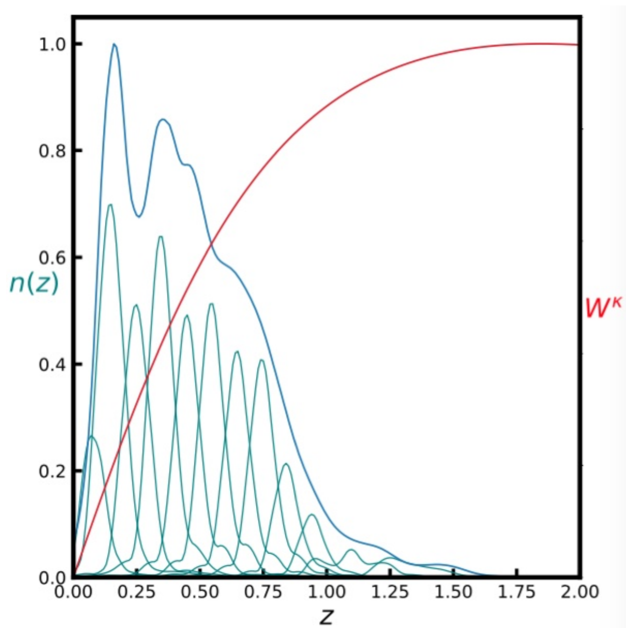

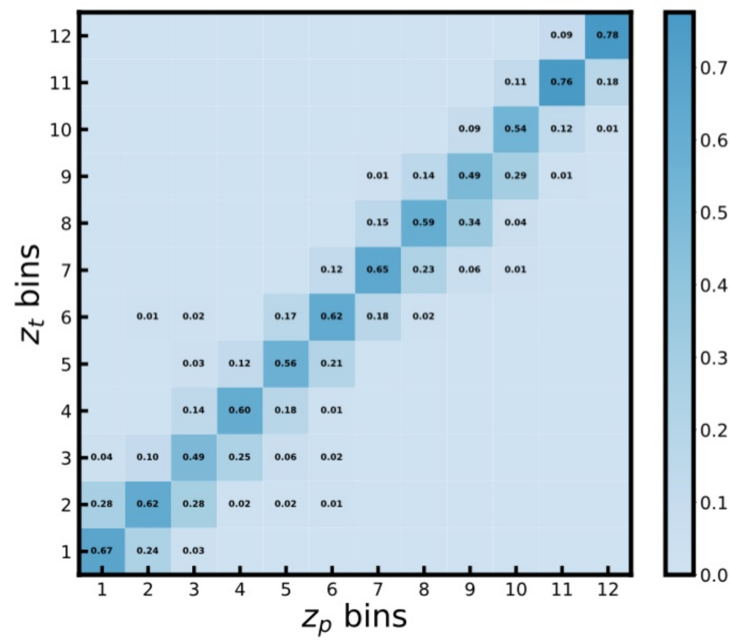

Credit: Ch. Saraf

Estimation of parameters

$$S_8 \equiv \sigma_8 \sqrt{\frac{\Omega_m}{0.3}}$$

$$S_8 = 0.832 \quad \text{(fiducial)}$$
$$S_8 = 0.792 \pm 0.013 \quad \text{(w/o corr)}$$
$$S_8 = 0.823 \pm 0.016 \quad \text{(with corr)}$$

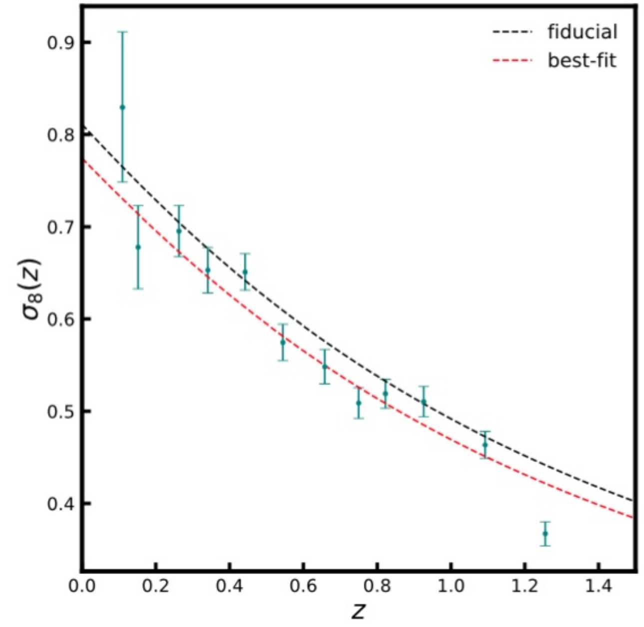

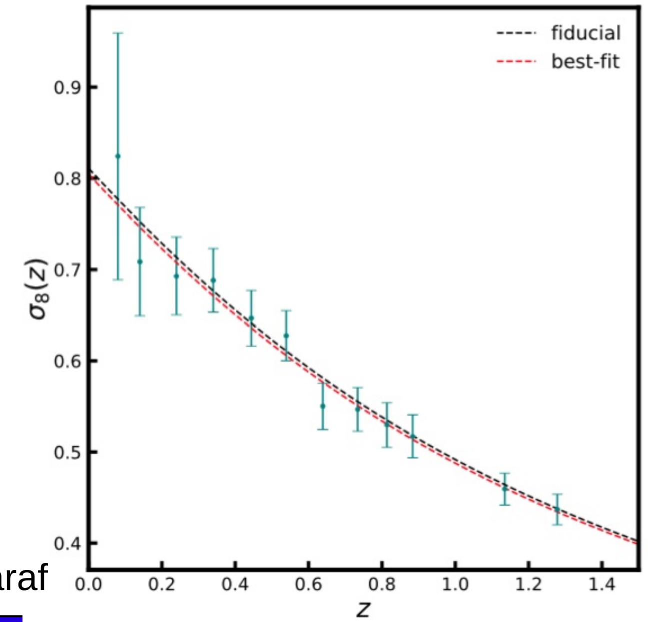

Credit: Ch. Saraf

Correlation with DESI Legacy Imaging Survey

- Cross-correlation between Planck CMB lensing potential and DESI Legacy Imaging Survey (DESI-LIS)

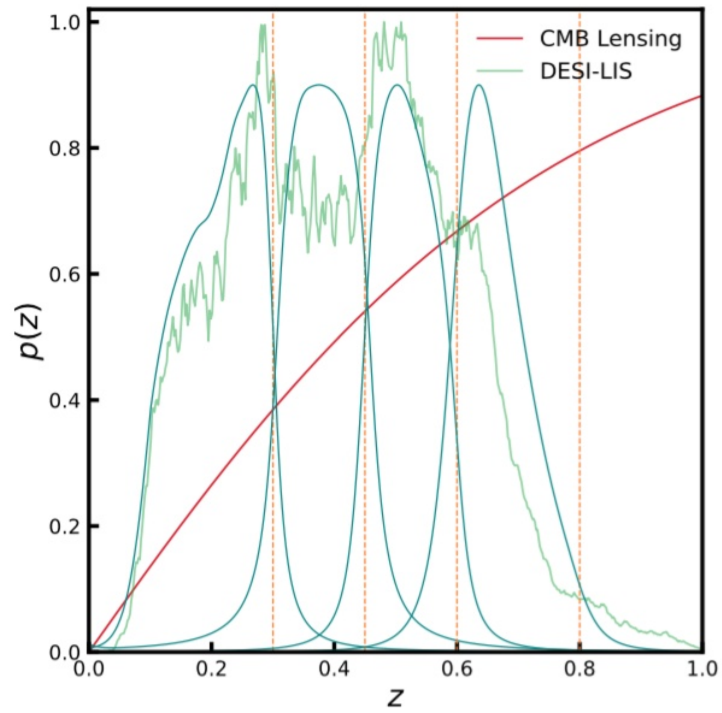

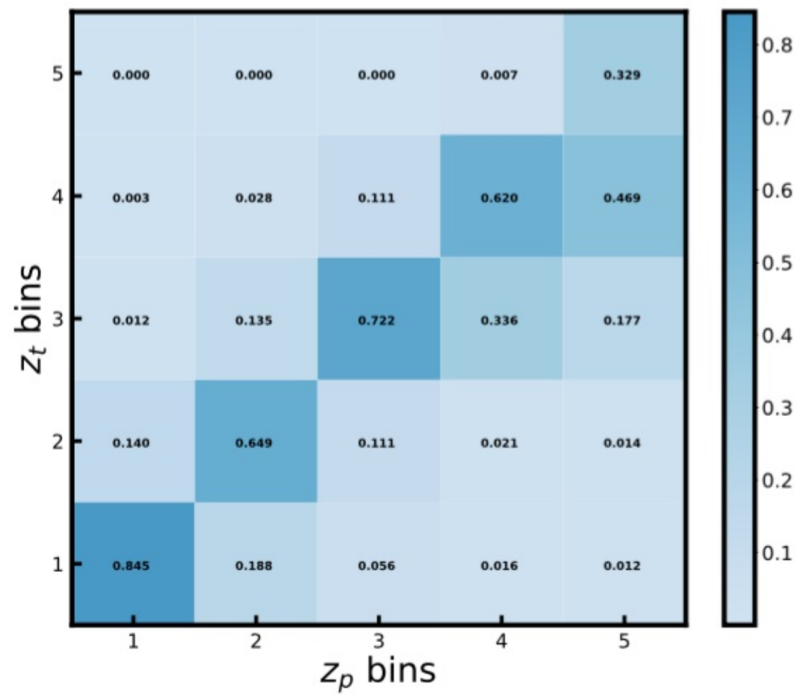

Saraf et al. (2024)

Correlation with DESI Legacy Imaging Survey

- Cross-correlation between Planck CMB lensing potential and DESI Legacy Imaging Survey (DESI-LIS)
- The clustering amplitude more consistent with the ΛCDM model after correction for the redshift bin mismatch (though deviation still present for the first two bins)

$$\sigma_8(z) = A(z)\,\sigma_{8,0}\,D(z)$$

$0 < z \leq 0.3$
$\sigma_8 = 0.731$ (fiducial)
$\sigma_8 = 0.623 \pm 0.045$ (w/o corr)
$\sigma_8 = 0.669 \pm 0.044$ (with corr)

$0.3 < z \leq 0.45$
$\sigma_8 = 0.664$ (fiducial)
$\sigma_8 = 0.501 \pm 0.032$ (w/o corr)
$\sigma_8 = 0.524 \pm 0.034$ (with corr)

$0.45 < z \leq 0.6$
$\sigma_8 = 0.618$ (fiducial)
$\sigma_8 = 0.530 \pm 0.030$ (w/o corr)
$\sigma_8 = 0.581 \pm 0.029$ (with corr)

$0.6 < z \leq 0.8$
$\sigma_8 = 0.577$ (fiducial)
$\sigma_8 = 0.483 \pm 0.024$ (w/o corr)
$\sigma_8 = 0.582 \pm 0.029$ (with corr)

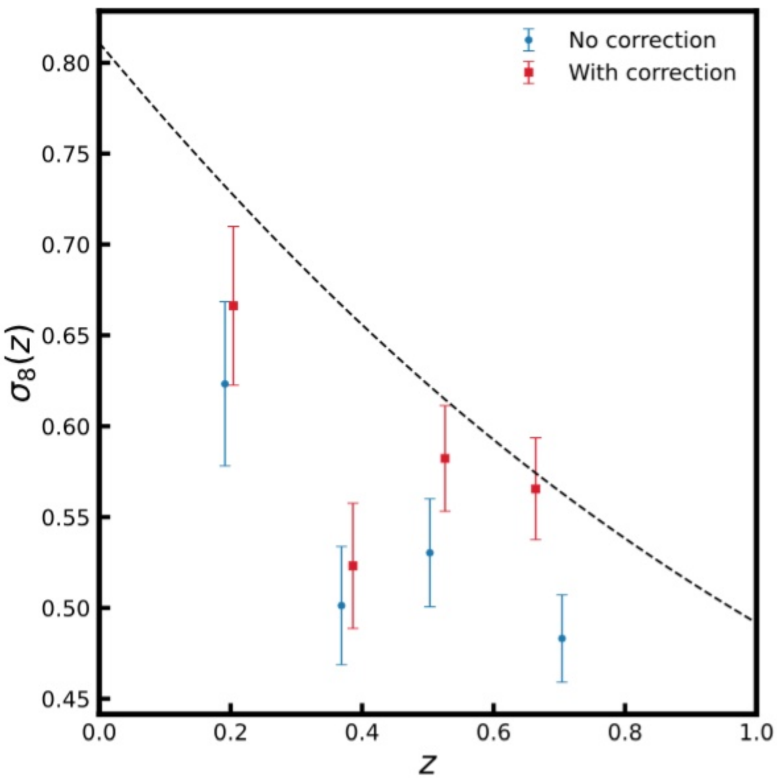

Saraf et al. (2024)

NARODOWE CENTRUM BADAŃ JĄDROWYCH ŚWIERK

Conclusions

- Tomographic cross-correlation between CMB lensing map and LSST galaxy survey useful for tracing time evolution of the large-scale structure
- Systematic errors caused by redshift bin mismatch of galaxies with photo-z
- ~3σ deviation on S_8 parameter due to bin mismatch for LSST Y1 simulations
- Needed correction for the redshift bin mismatch using scattering matrix formalism
- Potential solution to the S_8 tension in cosmology ?